

Effect of a thin spreading solvent film on the efficiency of the hexadecan-1-ol monolayer deposited for water evaporation retardation

Wu Yan,^{a*} Jia Qingzhu,^b Wang Bingwen,^a Zheng Wei,^a and Yi Shouzhi^a

^aSchool of Materials Science and Chemical Engineering, Tianjin University of Science and Technology, 300457 Tianjin, P.R. China.

Tel.: +86 (022) 606 00 029. E-mail: wuyantust@126.com

^bSchool of Marine Science and Engineering, Tianjin University of Science and Technology, 300457 Tianjin, P.R. China

The influence of a thin spreading solvent film (ethanol, diethyl ether, and three fractions of petroleum ether boiling at 30–60 °C, 60–90 °C, and 90–120 °C) on the properties of hexadecan-1-ol (C₁₆H₃₃OH) monolayers at the air–water interface was studied. The specific evaporation resistance and the surface pressure were determined to describe the spreading behavior of the C₁₆H₃₃OH monolayers. The physical properties of the solvents and the images obtained in an atomic force microscope were examined. The time of establishing the equilibrium spreading surface pressure of monolayers can be reduced using a more volatile solvent with a lower boiling point and a lower relative density. The influence of the monolayer nature on water evaporation corresponds to the order of changing the solvent spreading rate: petroleum ether (30–60 °C) > diethyl ether > ethanol > petroleum ether (60–90 °C) > petroleum ether (90–120 °C). The monolayers formed upon petroleum ether (30–60 °C) spreading form a film with a less deficient and relatively planar surface. When ethanol is used as a spreading solvent, water evaporation is accelerated rather than retarded, while petroleum ether (30–60 °C) is more appropriate for this purpose.

Key words: hexadecan-1-ol, monolayers, solvents, specific evaporation resistance, surface pressure, atomic force microscopic images.

Large areas, such as Western China, have experienced drought conditions over the past decades because of decreased rainfalls. As a consequence, efficient use of the limited available water in arid climates is highly desirable, but large amounts of water are frequently lost mainly owing to evaporation from open water storages. Researchers have shown that water evaporation can considerably be reduced by spreading water-insoluble monolayers of fatty acids and long-chain alcohols over the water surface.^{1–6} Moreover, it was revealed that the evaporation rate decreased with the elongation of the alkyl moiety or an increase in the intensity of interactions between alkan-1-ol molecules in the insoluble monolayer.⁷ A linear relationship was found between the logarithm of the specific evaporation resistance and inverse absolute temperature.^{4,5,8} Many available studies reported the physical properties of binary monolayers of simple long-chain compounds, such as alcohols, esters, amines, or other surfactants at the air–water interface.^{9–11}

Usually, investigations of monomolecular layers are carried out by spreading a surfactant insoluble in the solvent over the water surface. However, the most part of

previous studies paid much attention to the monolayer material. Only few studies systematically dealt with the effect of the spreading solvent on the evaporation rate and monolayer spreading.^{1,12}

The first assumptions about the influence of various volatile water-insoluble solvents on the properties of monolayers at the air–water interface had been published at the mid-20th century.¹ Solvents and substances after deep purification were used in the later studies.¹² It was revealed that the film substance was partially dissolved in the subphase if ethanol or mixtures with ethanol are used as the solvent spreading over the water surface. The intensity of film dissolution can be decreased due to using syringes with smaller needles. Although the IR spectra provide information on the conformational ordering and arrangement of molecules in the films, additional studies are necessary to refine the structural morphological organization of the films.

In the present study, a structural morphological approach to investigation of the effect of the solvent spreading rate on the properties of monolayers was proposed. The experiments were carried out with ethanol and diethyl

and petroleum ether films using saturated hexadecan-1-ol ($C_{16}H_{33}OH$) as a film-forming substance. The following parameters were determined to describe $C_{16}H_{33}OH$ monolayer spreading: spreading coefficient (S), specific evaporation resistance (r), water evaporation resistance (X), surface pressure (π), and physical properties of the solvents. The monolayer microstructure was studied by atomic force microscope (AFM).

Experimental

Materials. Hexadecan-1-ol (m.p. 49.2–49.6 °C) was purified by recrystallization from an *n*-hexane solution, and the purity was tested by melting point determination and gas chromatography (GC). The solvents were twice-distilled ethanol (fraction 78.4 °C), diethyl ether (fraction 34.5 °C), and petroleum ether (three fractions: 30–60 °C, 60–90 °C, and 90–120 °C), all solvents being analytically pure grade. The main physical properties of the solvents are given in Table 1. The water subphase was obtained by double distillation using a Pyrex distillation apparatus. Water quality was monitored by extraction with hexane followed by GC analysis.

Spreading technique. Water-insoluble monolayers were spread on the water surface from dilute solutions.^{3,13} Spreading solution droplets were distributed over the whole surface area of the cell. Before starting the experiment, the solvent was allowed to evaporate for 30 min. The system was placed in a water bath at a constant temperature of 25±0.5 °C. The scheme of the film localized at the air–water interface is shown in Fig. 1.

Specific evaporation resistance. The rate of evaporation from the water surface was measured by an increase in the weight of lithium chloride used as desiccant. At first lithium chloride was heated at 105 °C for water removal and then stored for a certain time at a distance of 2 mm from the water surface. The specific evaporation resistance (r) was determined by the equation^{1,2}:

$$r = A(w - w_0)(t/m_f - t/m_0), \quad (1)$$

where m_f and m_0 are the amount of water vapor absorbed within time t in the presence and in the absence of the monolayer on the water surface, respectively; w and w_0 are the concentrations of water vapor equilibrated with the water surface and desiccant, respectively; A is the water surface area covered with the desiccant. The w and w_0 values used were accepted as equal to $23.03 \cdot 10^{-6}$ and $2.33 \cdot 10^{-6}$ g mL⁻¹, respectively.

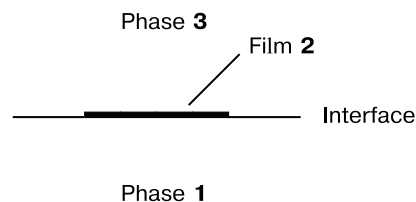


Fig. 1. Scheme of film 2 localized at the interface of phases 1 and 3.

Surface pressure. The surface pressure (π) was determined by the equation⁹:

$$\pi = \gamma_0 - \gamma, \quad (2)$$

where γ and γ_0 are the surface tension values in the presence and in the absence of the monolayer at the air–water interface, respectively.

Isotherms "surface pressure—surface area per molecule." The isotherms in the "surface pressure—surface area per molecule" coordinates (π — A isotherms) were measured at 25 °C with a KSV1100 automatic Langmuir–Adam haul-film balance. At first, a certain amount of a spreading solution was added with a microsyringe to the slot of the automatic balance. After 15 min, i.e., after processes of surface diffusion and solvent spreading and evaporation on the surface completed, the pressure was measured and the isotherm in the π — A coordinates was plotted. The temperature of the aqueous subphase was maintained constant (25±0.2 °C) using a thermostat with circulating water.

Spreading coefficient. If a drop of the liquid (2) is placed on the water surface (in our experiment, at the air–water (3/1) interface), the possibility of spontaneous spreading depends in the spreading coefficient (S) value of liquid 2. The S coefficient can be expressed as follows¹⁴:

$$S_{2(3/1)} = \gamma_{13} - \gamma_{12} - \gamma_{23} = \gamma_{13} - \gamma_{1(2)3}, \quad (3)$$

where γ_{ij} is the surface tension of the phases i and j ; $\gamma_{1(2)3}$ is the interface surface tension of film 2 covering the interface of phases 1 and 3. Thus, γ_{13} denotes the surface tension of water equal to 72 mN m⁻¹. If S is positive, liquid 2 can spread spontaneously at the interface of phases 1 and 3.

AFM images. The microstructure of monolayers was studied by atomic force microscopy (AFM) on a JSPM-5200 instrument. The monolayer was prepared for investigation by the horizontal lifting method using mica as a supporting solid substrate. The topography of the monolayers was observed by AFM at 298.2±2 K in a tapping mode, providing both a topographic

Table 1. Main physical properties of the solvents studied

Solvent	Ethanol ^a	Diethyl ether ^b	Petroleum ether, fractions		
			30–60 °C	60–90 °C	90–120 °C
Relative density (25 °C)	0.7893	0.7135	0.6372	0.6535	0.6743
Solubility in water	Soluble	Insoluble	Insoluble	Insoluble	Insoluble

^a B.p. 78.4 °C.

^b B.p. 34.5 °C.

image and phase contrast. The Si_3N_4 tips on integral cantilevers were used in the tapping mode at a scanning range of 1 μm .

Results and Discussion

Spreading coefficient. The spreading coefficient value (S) is very important for analysis of the spreading rate of the monolayer with the solvent over the water surface. The coefficient describes both the possibility of spontaneous spreading and relative differences between spreading of the monolayers obtained from various solvents. The data in Table 2 indicate that at positive S values all spreading solutions can spontaneously form a film at the air–water interface. The difference between the behaviors of various solutions shows that the spreading rate of the solvent significantly affects the film-forming ability. The spreading ability order for the solvents studied is as follows: petroleum ether (30–60 °C) > diethyl ether > ethanol > petroleum ether (60–90 °C) > petroleum ether (90–120 °C).

Isotherms in the π – A coordinates. The isotherms for the $\text{C}_{16}\text{H}_{33}\text{OH}$ monolayers in the π – A coordinates are shown in Fig. 2. All isotherms are similar in shape, especially those for the monolayers obtained from diethyl ether and diethyl ether (30–60 °C). Figure 2 shows that, when using various solvents, $\text{C}_{16}\text{H}_{33}\text{OH}$ can form incompressible films. However, the spreading rates of the monolayers from diethyl ether or petroleum ether (30–60 °C) and ethanol differ noticeably. The reason is that the molecules of diethyl and petroleum (30–60 °C) ethers squeeze out from the monolayer more rapidly due to lower boiling points and higher volatilities than those of ethanol. Petroleum ether (30–60 °C) molecules with a lower density are removed especially rapidly. Therefore, the monolayers spreading from petroleum ether (30–60 °C) are characterized by the highest cohesion work and the smallest (about 0.191 nm^2) surface area per molecule.

Isotherms in the π – t coordinates. The surface pressure (π) exerts a strong effect on the retardation of water evaporation. The higher the surface pressure, the stronger the cohesion work in the monolayers. Therefore, the change in the surface pressure with time for monolayers can be used for studying the distribution and pervasion of a film-forming material into the surface layer of water.

In this work, the change in π value with time (t) for the monolayers was studied under atmospheric pressure, which

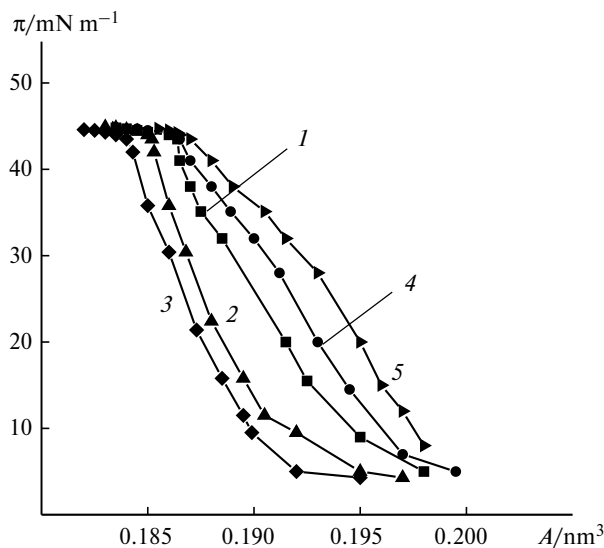


Fig. 2. Isotherms in the π – A coordinates for the $\text{C}_{16}\text{H}_{33}\text{OH}$ monolayers obtained from various spreading solvents: ethanol (1), diethyl ether (2), and three fractions of petroleum ether: 30–60 °C (3), 60–90 °C (4), and 90–120 °C (5).

makes it possible to determine the equilibrium surface spreading pressure (ESP) and the time of equilibration. The results presented in Fig. 3 show that π increases rapidly during the short initial period and then continues to increase very slowly. This agrees with the theoretical assumptions that the surface pressure tends to achieve more or less constant value.¹⁵

However, the behaviors of the monolayers obtained from various solvents differ. As follows from Fig. 3, if diethyl ether and petroleum ether (30–60 °C) are used as solvents, the metastable equilibrium is achieved rather quickly, and the equilibrium pressure is detected already in ~80 min. At the same time, in the case of ethanol, the ESP is achieved only after ~200 min, whereas for petroleum ether (90–120 °C) the equilibration is achieved after ~250 min.

Therefore, it can be concluded that the rate of achievement of the monolayer ESR is related to the physical properties of spreading solvents, such as the boiling point, volatility, and density. The achievement of the equilibrium surface pressure of monolayers can be accelerated due to the use of a solvent with a higher volatility and lower boiling point and relative density.

Table 2. Spreading coefficients ($S_{2(3/1)}$) of the solvents and the interfacial surface tension ($\gamma_{1(2/3)}$) of the film at the air–water interface

Parameter	Ethanol	Diethyl ether	Petroleum ether, fractions		
			30–60 °C	60–90 °C	90–120 °C
$\gamma_{1(2/3)}/\text{mN m}^{-1}$	50.7	49.7	46.8	53.2	60.7
$S_{2(3/1)}/\text{mN m}^{-1}$	21.3	22.3	25.2	18.8	11.3

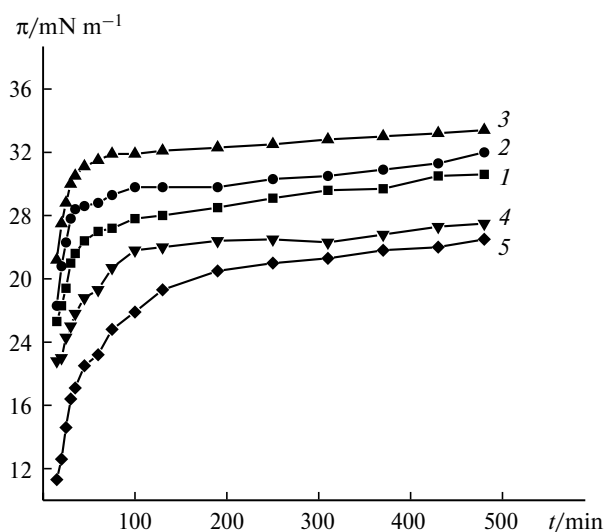


Fig. 3. Change in the surface spreading pressure of the $C_{16}H_{33}OH$ monolayers in time for various spreading solvents: ethanol (1), diethyl ether (2), and three fractions of petroleum ether: 30–60 °C (3), 60–90 °C (4), and 90–120 °C (5).

Isotherms in the r – t coordinates. The results of studies of the effect of various spreading solvents on the character of the isotherms plotted in the "specific evaporation resistance—time" coordinates are presented in Fig. 4. It can be seen that at the initial time period the effects of retardation of the evaporation rate by the monolayers obtained from various solvents are very small and r is only ~ 0.2 . Then r increases rapidly and after some time achieves a constant value. Among the three systems studied containing petroleum ethers, a comparatively constant r value was detected most quickly (after 80 min) for petroleum ether boiling at 30–60 °C. The longer time (120 min) was needed in experiments with petroleum ether boiling in the range 60–90 °C. The achievement of a constant r value took the longest time (almost 250 min) in experiments with petroleum ether boiling at 90–120 °C. The systems stabilized completely after 480 min, and the r value for petroleum ether (30–60 °C) was 1.31, while it decreases to 0.86 and 0.68 for petroleum ethers (60–90 °C) and (90–120 °C), respectively. The effect evaporation retardation for five monolayer samples decreases in the following order: petroleum ether (30–60 °C) > diethyl ether > ethanol > petroleum ether (60–90 °C) > petroleum ether (90–120 °C). The differences in the character of the dependences of r on t can be due to the fact that some solvent molecules are first retained in the $C_{16}H_{33}OH$ monolayer formed upon film spreading. The gradual "squeezing out" of these molecules from the dense film packing increases r with time. Therefore, the results presented in Fig. 4 suggest that various solvents are characterized by different r values and the reason lies, first of all, in a large difference in the boiling points and volatilities of the solvents.

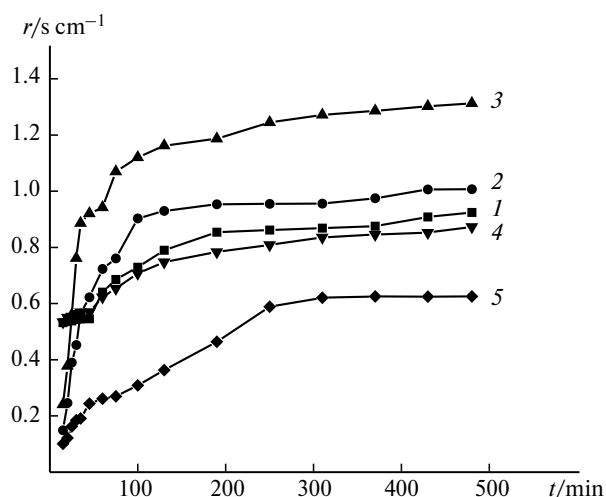


Fig. 4. Change in the specific resistance of the $C_{16}H_{33}OH$ monolayers in time for various spreading solvents: ethanol (1), diethyl ether (2), and three fractions of petroleum ether: 30–60 °C (3), 60–90 °C (4), and 90–120 °C (5).

Effect of foreign molecules. Resistance of the monolayers is related to the energy necessary for the formation of a vacancy in the film. Therefore, the presence of small amounts of solvent and foreign molecules can exert a rather strong effect on the retardation of water evaporation, since these molecules form vacancies in the insoluble monolayers.¹

In order to interpret the effect of solvent spreading on retardation of water evaporation by monolayers, one can use the equation¹ that describes the resistance of hexadecan-1-ol molecules to the presence of obstructed solvent molecules

$$1/r = 1/r_{C_{16}H_{33}OH} + n_0/r_0, \quad (4)$$

where $r_{C_{16}H_{33}OH}$ is the specific resistance of $C_{16}H_{33}OH$ in the absence of the inclusion effect of obstructed solvent molecules equal to 1.4 s cm⁻¹ (see Ref. 2), n_0 is the mole fraction of obstructed solvent molecules, and r_0 is the specific resistance of free sites occupied by obstructed solvent molecules equal to $1.9 \cdot 10^{-3}$ s cm⁻¹ (see Ref. 1).

In this study, the mole fraction of obstructed solvent molecules was calculated by Eq. (4) from the experimental values of specific resistance detected after 8 h. The corresponding results are listed in Table 3. The calculations show that the mole fraction of solvent molecules obstructed in the monolayers for petroleum ether (30–60 °C) is much smaller than for other solvents. Petroleum ether (30–60 °C) molecules cannot be retained in the monolayers due to its lower boiling point and insolubility in water and, thus, they cannot affect their compressibility. In addition, the density of petroleum ether (30–60 °C) is the lowest compared to those of other solvents, which can decrease solvent sinking into the subphase of water and, therefore, the character of the water subphase remains unchanged and does not prevent film

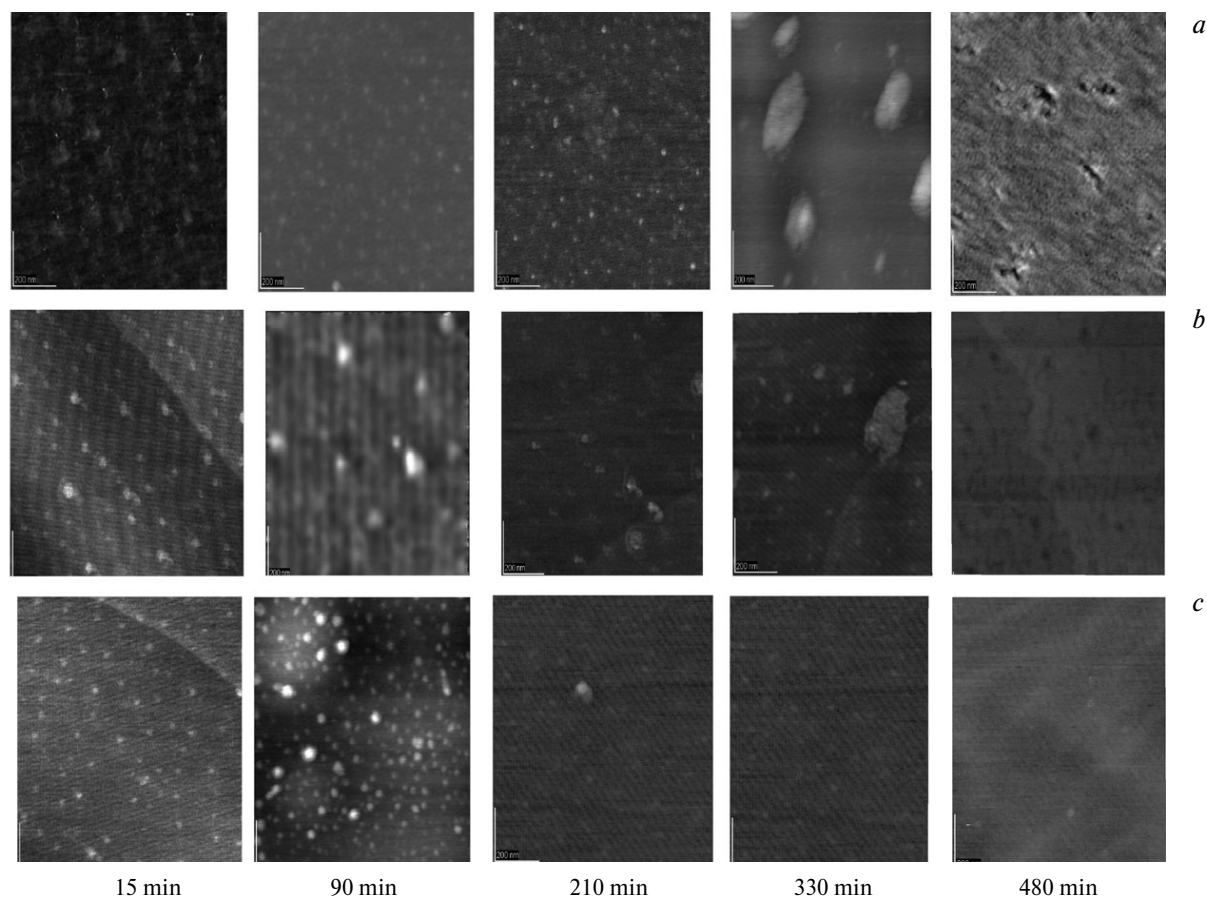
Table 3. Specific resistance (r_0) and mole fractions (n_0) of molecules obstructed in the monolayers obtained from various spreading solvents

Parameter	Ethanol	Diethyl ether	Petroleum ether, fractions		
			30–60 °C	60–90 °C	90–120 °C
$r_0/\text{s cm}^{-1}$	0.92	1.01	1.31	0.87	0.68
n_0	$0.71 \cdot 10^{-3}$	$0.52 \cdot 10^{-3}$	$0.93 \cdot 10^{-4}$	$0.83 \cdot 10^{-3}$	$1.44 \cdot 10^{-3}$

formation and the compression and resistance of the monolayers. That is why the best effect of retardation of the evaporation rate is observed for the monolayer obtained from petroleum ether (30–60 °C). This layer has the best spreading ability over the surface and contains the minimum number of obstructed solvent molecules.

Atomic force microscopic images. The AFM images ($1 \times 1 \mu\text{m}$) of the topography of the $\text{C}_{16}\text{H}_{33}\text{OH}$ monolayers transferred onto mica at the ESP at different times are shown in Figs 5 and 6. As can be seen from Fig. 5, some domains of the crystalline phase appear during the initial spreading period, and the monolayers are poorly ordered and loosely packed. They are dispersed with time and,

finally, it is visible that the monolayer on the water surface becomes homogeneous, although the pattern differs for various solvents. Figure 6, *a* shows that the $\text{C}_{16}\text{H}_{33}\text{OH}$ monolayers contain defect wells 4.1 nm in depth, whereas the monolayer obtained from an ethanolic solution contain elliptical voids 10–100 nm in diameter, which can be ascribed to the presence of solvent molecules in the monolayer. In the case of the monolayers from diethyl ether and petroleum ether (30–60 °C), a relatively flat topography with a less deficient surface can be observed (see Fig. 6, *b, c*), although the monolayer obtained from diethyl ether has no homogeneity characteristic of the layer obtained from petroleum ether (30–60 °C).

**Fig. 5.** The AFM images (scale $1 \times 1 \mu\text{m}$) obtained at 25 °C 15–480 min after the $\text{C}_{16}\text{H}_{33}\text{OH}$ monolayers were transferred onto mica from ethanol (*a*), diethyl ether (*b*), and petroleum ether (30–60 °C) (*c*).

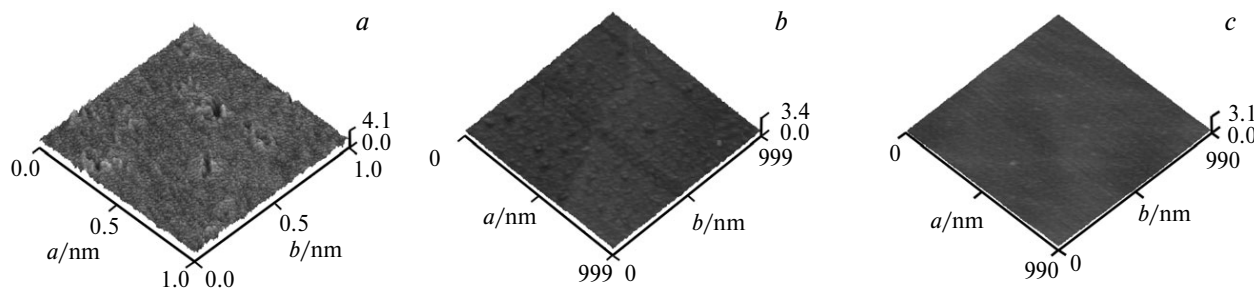


Fig. 6. The AFM images (scale $1 \times 1 \mu\text{m}$) and the data on the height obtained at 25°C 480 min after the $\text{C}_{16}\text{H}_{33}\text{OH}$ monolayers were transferred onto mica from ethanol (a), diethyl ether (b), and petroleum ether ($30\text{--}60^\circ\text{C}$) (c).

* * *

References

Therefore, we studied the spreading effect of ethanol, diethyl ether, and petroleum ether (fractions boiling at $30\text{--}60^\circ\text{C}$, $60\text{--}90^\circ\text{C}$, and $90\text{--}120^\circ\text{C}$) on the properties of the hexadecan-1-ol monolayers at the air–water interface. The results showed that the rate of achievement of the equilibrium surface spreading pressure of the monolayers can be increased using a solvent that better spreads over the surface and has a higher volatility and reduced boiling point and density. All AFM images show that with time the monolayers in the water surface become homogeneous and the monolayers obtained from petroleum ether ($30\text{--}60^\circ\text{C}$) can form a film with a less deficient and relatively flat surface. The combined analysis of the isotherms plotted in the coordinates $\pi\text{--}A$, $\pi\text{--}t$, $r\text{--}t$, and $X\text{--}t$ and the AFM images suggests that ethanol used as the solvent does not decrease and, on the contrary, enhances the evaporation rate. Petroleum ether (fraction $30\text{--}60^\circ\text{C}$) turned out to be the most promising spreading solvent.

So, the properties of the monolayers at the air–water interface depend strongly on the nature of the thin spreading solvent film. The better the solvent spreading, the more efficient the retardation of water evaporation by the monolayer.

This work was financially supported by the Tianjin Natural Science Foundation (Grant 09JCYBJC06100) and the Foundation of Tianjin Science and Technology Development Program (Grant 20 060 513).

1. R. J. Archer, V. K. La Mer, *J. Phys. Chem.*, 1955, **59**, 200.
2. I. Langmuir, V. J. Schaefer, *J. Franklin Inst.*, 1943, **235**, 119.
3. V. K. La Mer, T. W. Healy, L. A. G. Aylmore, *J. Colloid Sci.*, 1964, **19**, 673.
4. G. T. Barnes, *Colloids Surf. A: Physicochem. Eng. Aspects*, 1997, **126**, 149.
5. M. Tsuji, H. Nakahara, Y. Moroi, O. Shibata, *J. Colloid Interface Sci.*, 2008, **318**, 322.
6. G. T. Barnes, *Agr. Water Manage.*, 2008, **95**, 339.
7. M. Rusdi, Y. Moroi, *J. Colloid Interface Sci.*, 2004, **272**, 472.
8. G. T. Barnes, *Adv. Colloid Interface Sci.*, 1986, **25**, 89.
9. S. Machida, M. Shoko, F. Atsuhiko, H. Nakahara, *J. Colloid Interface Sci.*, 2003, **260**, 135.
10. S. Machida, H. Nakahara, I. Yoshikawa, Y. Shibasaki, K. Fukuda, *Thin Solid Films*, 1998, **327–329**, 109.
11. C. E. McNamee, G. T. Barnes, I. R. Gentle, J. B. Peng, R. Steitz, R. Probert, *J. Colloid Interface Sci.*, 1998, **207**, 258.
12. A. Gericke, J. Simon-Kutscher, H. Huehnerfuss, *Langmuir*, 1993, **9**, 2119.
13. G. T. Barnes, D. S. Hunter, *J. Colloid Interface Sci.*, 1990, **136**, 198.
14. Z. X. Zhonghuan, Z. Yan, S. S. Xu, P. Z. Lang, *Physics and Chemistry of Films*, Science Press, China, 1997.
15. T. Sugama, J. E. DuVall, *Thin Solid Films*, 1996, **289**, 39.

Received August 5, 2009